



Article

Toxicological Effects of Inorganic Nanoparticle Mixtures in Freshwater Mussels

Joelle Auclair ¹, Patrice Turcotte ¹, Christian Gagnon ¹, Caroline Peyrot ², Kevin J. Wilkinson ² 
and François Gagné ^{1,*} 

¹ Aquatic Contaminants Research Division, Environment and Climate Change Canada, Montreal, QC H2Y 2E7, Canada; joelle.auclair@canada.ca (J.A.); patrice.turcotte@canada.ca (P.T.); christian.gagnon@canada.ca (C.G.)

² Department of Chemistry, Montréal University, Montréal, QC H2V 2B8, Canada; Caroline.peyrot@umontreal.ca (C.P.); kj.wilkinson@umontreal.ca (K.J.W.)

* Correspondence: francois.gagne@canada.ca

Received: 22 October 2020; Accepted: 9 December 2020; Published: 12 December 2020



Abstract: The toxicological effects of nanoparticles mixtures in aquatic organisms are poorly understood. The purpose of this study was to examine the tissue metal loadings and sublethal effects of silver (nAg), cerium oxide (nCeO), copper oxide (nCuO) and zinc oxide (nZnO) nanoparticles individually at 50 µg/L and in two mixtures to freshwater mussels *Dreissena bugensis*. The mixtures consisted of 12.5 µg/L of each nanoparticle (Mix50) and 50 µg/L of each nanoparticles (Mix200). After a 96-h exposure period, mussels were analyzed for morphological changes, air time survival, bioaccumulation, inflammation (cyclooxygenase or COX activity), lipid peroxidation (LPO), DNA strand breaks, labile Zn, acetylcholinesterase (AChE) and protein–ubiquitin levels. The data revealed that mussels accumulated the nanoparticles with nCeO and nAg were the least and most bioavailable, respectively. Increased tissue metal loadings were observed for nCeO and nCuO in mixtures, while no mixture effects were observed for nAg and nZnO. The weight loss during air emersion was lower in mussels exposed to nCuO alone but not by the mixture. On the one hand, labile Zn levels was increased with nZnO but returned to control values with the Mix50 and Mix200, suggesting antagonism. On the other hand, DNA strand breaks were reduced for both mixtures compared to controls or to the nanoparticles individually, suggesting potentiation of effects. The same was found for protein–ubiquitin levels, which were decreased by nCeO and nCuO alone but not when in mixtures, which increased their levels. In conclusion, the data revealed that the behavior and effects of nanoparticles were influenced by other nanoparticles where antagonist and potentiation interactions were identified.

Keywords: nanoparticles; mixtures; labile zinc; ubiquitin; oxidative stress; DNA damage

1. Introduction

The nanotechnology industry is a sector of intense development leading to the inadvertent release of various nanoparticles in the environment. Nanotechnology has found applications in many areas of consumer products and technology such as microelectronics, bacteriostatic agents in medical device and clothing, drug vectors, medical imaging, fuel additives and materials (ceramics). Among the inorganic nanoparticles, elemental and metal oxides nanoparticles such as cerium oxide (nCeO₂), copper oxide (nCuO), silver (nAg) and zinc oxide (nZnO) are often found in the environment and could reach the aquatic biota [1–3]. In the environment, these nanoparticles find their way in municipal effluents where organisms are likely exposed to mixtures of nanoparticles in addition to other contaminants usually found in municipal effluents [4]. nAg have interesting antimicrobial properties, as with nZnO,

and they are embedded in many consumer products such as clothes, shoes, masks and sport wares, thereby limiting fouling and odors [5], and are commonly found in municipal effluents [6] (Polesel et al., 2018). Cerium oxide nanoparticles (nCeO₂) are widely used in biomedical sector as antioxidants in biological systems, fuel additives and ceramic applications [7–9]. Hence, cerium pollution occurs mainly with solid landfills and leachates of electronic devices, sludge and wastewaters from ceramic plant industries. Copper oxide nanoparticles are currently used in cosmetics, catalysts, gas sensors, and in microelectronic materials [10]. The strong UV absorption of zinc oxide nanoparticles makes them popular sunscreens [11]. Sunscreen lotions are usually composed of bulk zinc oxide suspensions forming a white paste on the skin, while nZnO-based lotions are transparent while maintaining their UV screening effects. This nanoparticle also has antimicrobial properties, which is an additional benefit.

Most studies dealing with the toxicity of nanoparticles focused on the intrinsic toxicity of a single nanoparticle and compared it with the dissolved element counterpart (Cu(II) vs. nCuO) in terms of size and coating effects. However, there is a lack of studies dealing with the toxicity of mixtures of nanoparticles in aquatic organisms, especially for mussels. Mussels were recognized as relevant models for nanomaterials given their lifestyles, such as sessility and feeding on suspended materials including nanoparticles and aggregates [12,13]. Moreover, toxicity data for this group of invertebrates are lacking compared to other taxonomic groups such as fish, algae and microcrustaceans. For example, nCuO toxicity was about six times less toxic than Cu(II) in rainbow trout [14,15]. The 96-h lethal concentration of Cu (II) was 120 µg/L compared to 680 µg/L for nCuO in rainbow trout. The acute toxicity distribution 5th percentile threshold (HC5) was 10 and 150 µg/L for Cu(II) and nCuO, respectively, and 30 and 60 µg/L for Zn(II) and nZnO, respectively [16]. Hence, these nanoparticles are much less toxic than the dissolved components. The 96-h acute toxicity of nCuO in neotropical fish *Hyphessobrycon eques* was estimated at 210 µg/L compared to 50 µg/L for nCuO and Cu(II) [17]. Studies dealing with mixtures of nanoparticles are scarce. A recent study investigated the toxicity of nCuO in the presence of nZnO in rainbow trout [18]. The acute 96-h LC50 for nZnO was 3 and > 0.34 mg/L for nCuO in rainbow trout. The toxicity (LC50) of nCuO in the presence of non-toxic concentration of nZnO (NOEC = 1.25 mg/L for survival) was increased with an LC50 of 0.1 mg/L, highlighting a mixture interaction. The hepatic Cu and Zn contents were increased when nCuO was co-exposed with nZnO. The fish in the co-exposure treatment group had increased glutathione S-transferase activity and the GSH/GSSG ratio was increased at low nCuO concentration followed by a decrease at higher concentrations in the presence of nZnO. This suggests that the tissue metal loadings and toxicity of nanoparticles could be influenced by other nanoparticles.

The purpose of this study was therefore to determine the tissue metal loadings and toxic effects of four commonly found elemental nanoparticles in freshwater mussel *Dreissena bugensis* individually, and in two mixtures at environmentally relevant concentrations. The mussels were exposed individually to nAg, nCeO, nCuO and nZnO and in mixture for 96 h at 15 °C. Morphological changes and physiological stress were determined, along with a test battery of biomarkers of stress related to oxidative stress, inflammation, Zn homeostasis, DNA damage and damaged protein turnover. An attempt was made to identify mixture interactions of commonly used nanoparticles with mussels.

2. Material and Methods

All four nanoparticles (cerium, copper, silver and zinc) in this study were obtained as water-based suspensions to minimize the handling risk of fine powders. Cerium dioxide (nCeO₂) and zinc oxide (nZnO) nanoparticles were obtained from Sigma-Aldrich (Oakville, ON, Canada). According to the manufacturer's certificate of analysis, the mean diameter for each nanoparticle were <25 and <100 nm, respectively. Commercially available, 50-nm, citrate-coated silver nanospheres (nAg) were purchased from nanoComposix Inc. (San Diego, CA, USA). A stock of copper oxide (nCuO) nanoparticles with a diameter range of 25–55 nm was obtained from US Research Nanomaterials (Houston, TX, USA).

Specimens of *Dreissena bugensis*, quagga mussels, were collected from the Saint-Laurence River (Point-des-Cascade, Canada) by gently cutting off their attached byssus from the wall of the Soulanges

canal and transported to the laboratory at 4 °C in coolers. Prior to any exposure, mussels were acclimated for a minimum of two weeks during which time they were maintained at 15 °C in 20-L of dechlorinated and UV-treated tap water under constant aeration and following a 16-h light: 8-h dark photoperiod. Mussels were fed three times a week with the combination of phytoplankton (Phytoplex, Kent Marine, WI, USA) and *Pseudokirchneriella subcapitata* algal suspension at 100 million cells/100 mL concentration.

2.1. Experimental Design and Exposure Conditions

Assessment of the toxic effects of various nanoparticles (nAg, nCuO, nZnO and nCeO₂) and two mixtures was determined in the freshwater mussel *Dreissena bugensis*. The mussels were exposed to 50 µg/L of each nanoparticle and two mixtures with a control in 4-L containers containing 30 mussels each exposure group, i.e., six exposure groups (nanoparticles) and one control group. Each nanoparticle was diluted first to 10 mg/L in MilliQ water and then at 50 µg/L in aquarium water. Mixture 1 (MIX50) was composed of 12.5 µg/L of each nanoparticle (nAg, nCe, nCu and nZnO), giving a total of 50 µg/L. Mixture 2 (MIX200) was composed of 50 µg/L of each nanoparticle (nAg, nCe, nCu and nZnO), giving a total of 200 µg/L. The nanoparticle size distribution and Zeta potential were determined after 1 h in aquarium water using a dynamic light scattering instrument (Mobius Instrument, Wyatt Technologies, Santa Barbara, CA, USA) operating with a laser at a wavelength of 532 nm. The instrument was previously calibrated with standard suspensions of latex nanoparticles (Polyscience, Niles, IL, USA). The aquarium water consisted of tap water from the city of Montreal (QC, Canada), which was UV-treated and dechlorinated (conductivity: 250 µS cm⁻¹, pH = 7.8, organic carbon content: 5 mg/L and total suspended solids <1 mg/L).

Mussels were exposed to the nanoparticles individually and in two mixtures, as described below, for 96 h at 15 °C under constant aeration. Mussels were not fed during the exposure period and a semi-static mode was adopted with a complete renewal of all test solutions after 48 h. Basic water chemistry parameters (dissolved oxygen, pH, temperature and conductivity) were monitored for each treatment at different timepoints (0, 48 and 96 h) (Table 1). The study was designed to enable the comparison of nanoparticles individually with two different mixtures generated by the combination of the four metals simultaneously. In this study, 210 mussels with an average shell length of 26 ± 3 mm were randomly selected and exposed to seven different treatments (N = 30 mussels per treatment) including one control group in 4 L of aquarium water (dechlorinated and UV-treated tap water), four groups consisting of individual nanoparticles and two groups for the mixture 1 and 2. Treatments consisted of the exposure to nanoparticle alone (nAg, nCuO, nZnO and nCeO) at the fixed concentration of 50 µg/L and to two mixtures, one with a total metallic content of 50 µg/L (i.e., 12.5 µg/L per each nanoparticle) and another reaching a concentration of 200 µg/L in total metals (i.e., 50 µg/L per each nanoparticle). The selection of the 50 µg/L concentration was selected based on the observation that these elements are found in municipal effluents and combined sewer overflows at concentrations between 0.1 and 100 µg/L [19,20]. Hence, the concentration is at the upper limit (worst-case scenario) of these elements in municipal effluents. At the end of the assay, 10 mussels per group were collected and kept in clean water for an overnight depuration to be then stored at −85 °C for subsequent bioaccumulation analysis. The remaining mussels were divided in two subgroups for the air-time survival assessment (N = 10 mussels) and biomarkers analyses (N = 10 mussels) and stored at −85 °C.

2.2. Air Survival Test

The ability of mussels to withstand additional stress was evaluated by the air-time survival test at the end of the exposure. Briefly, 10 individuals were randomly collected for each exposure group and control. Initial weight and shell length were measured, then mussels were placed in their designated plastic weight boat. Exposure to air was conducted in an incubator under 80% humidity at 20 °C. Monitoring of weight loss and signs of mortality (opened shell or no reaction) were performed on a

daily basis. Air-time survival was expressed as the mean lethal time and the percentage weight loss per day at the time of death: $100 \times (\text{weight}_{T_0} - \text{weight}_{T_{\text{death}}}) / \text{weight}_{T_0}$.

Table 1. Physico-chemical properties of nanoparticles and their mixture.

Nanoparticle	Concentration	Mean Diameter (nm)	Zeta Potential (mV)	pH ¹	Conductivity ¹ $\mu\text{S} \times \text{cm}^{-1}$
Control	—	—	—	T ₀ : 7.9 48 h: 8.09 96 h: 8.11	T ₀ : 309 48 h: 312 96 h: 312
nAg	0.02 mg/mL (water)	51 + 6	−48	T ₀ : 8.0 48 h: 8.09 96 h: 8.14	T ₀ : 309 48 h: 314 96 h: 314
nCuO	20 mg/mL (water)	64 ± 2	−12.4	T ₀ : 7.95 48 h: 8.11 96 h: 8.14	T ₀ : 309 48 h: 311 96 h: 312
nCeO ₂	10 mg/mL (water)	47 ± 1	−14.7	T ₀ : 7.98 48 h: 8.1 96 h: 8.18	T ₀ : 309 48 h: 312 96 h: 312
nZnO	20 mg/mL (water)	63 ± 1	−22.6	T ₀ : 7.99 T _{48h} : 8.1 T _{96h} : 8.2	T ₀ : 309 T _{48h} : 312 T _{96h} : 312
Mix 1 50 µg/L	—	—	—	T ₀ : 8.0 T _{48h} : 8.1 T _{96h} : 8.2	T ₀ : 309 T _{48h} : 313 T _{96h} : 312
Mix 2 200 µg/L	—	—	—	T ₀ : 8.0 T _{48h} : 8.1 T _{96h} : 8.2	T ₀ : 309 T _{48h} : 313 T _{96h} : 313

¹ Measurement were made at 50 µg/L in aquarium water during the exposure experiments.

2.3. Bioaccumulation Determination

The total levels of Ag, Ce, Cu and Zn in the exposure water and in mussels were determined by high-resolution plasma mass spectrometry. For aquarium water, elements were determined after 1 h of dissolution in aquarium water following acidification with 1% *v/v* nitric acid (Seastar grade BC, Canada). Quagga mussels ($n = 10$ for each of the seven treatment groups) were exposed as described above for 96 h at 15 °C under constant aeration. The exposure media were not renewed and the mussels were not fed during that time. A subgroup of 10 individuals were placed in clean aquarium water overnight as a depuration step and the mussels were removed for elemental determination using ICP mass spectrometry (XSERIES 2 ICP-MS, Thermofisher Scientific, Waltham, MA, USA) using standard solutions of Ag, Ce, Zn and Cu chloride salts in 1% *v/v* nitric acid). The metal/element contents were determined in mussel individuals (no pooling of mussels). The tissues from each individual mussel were acid-digested with an equal volume (1 mL) of each of concentrated HNO₃ (16 N), HCl (12 N) and 30% H₂O₂, followed by heat-digestion in microwave vessels for 2 h, and diluted with MilliQ water to a volume of 12 mL. The total levels of metals/elements in mussel tissues were determined using ion-coupled plasma mass spectrometry, as described above, using standard solutions of Ag, Ce, Zn and Cu chloride salts in 1% *v/v* nitric acid.

2.4. Biochemical Profile Assessment

Mussels from thawed on ice and the shell length, total and soft-tissue weights were determined. The frozen soft tissues were immediately mixed with five volumes of ice-cold homogenization buffer (25 mM Hepes-NaOH, 100 mM NaCl, 0.1 mM dithiothreitol and 1 µg/mL aprotinin, pH 7.4) and homogenized on ice using a hand-held Polytron tissue grinder. A portion of the homogenate

was centrifuged at $15,000\times g$ for 20 min at $4\text{ }^{\circ}\text{C}$ and the resulting supernatant was collected (S15). Total protein contents were determined in both homogenate and S15 fraction by the protein dye binding assay with bovine serum albumin (BSA) for calibration [21].

Lipid peroxidation (LPO) was determined in tissue homogenates with a microplate version of the thiobarbituric acid (TBA) assay [22]. The reaction mixture consisted of homogenate mixed with trichloroacetic acid and TBA reagents in a volume ratio of 1:2:1, respectively in a total volume of $200\text{ }\mu\text{L}$. Thiobarbituric acid reactants (TBARS) were detected by fluorescence at 540 nm excitation/ 600 nm emission using a standard solution of tetramethoxypropane for calibration. Data were expressed as nmoles of TBARS/mg proteins.

DNA damage was also evaluated in the homogenate using an alkaline precipitation assay [23] and a fluorescent detection of DNA strand methodology [24]. The assay is based on the isolation and quantification of released DNA from impaired nucleoprotein structures (nucleosomes and mitochondrial nucleoids). DNA strands of the collected supernatant fraction were stained with the Hoechst dye and measured at 360 nm excitation and 460 nm emission (Microplate reader, Synergy-4, Biotek, Winooski, VT, USA). Salmon sperm DNA was used as standard and the data were expressed as $\mu\text{g DNA/mg proteins}$.

Displacement of essential metals by metal-based nanoparticles was measured by quantifying changes in labile Zn levels using a fluorescent probe methodology [25]. Briefly, $20\text{ }\mu\text{L}$ sample of the S15 fraction was mixed with $180\text{ }\mu\text{L}$ of $110\text{ }\mu\text{M}$ of TSQ probe in 20% DMSO in phosphate buffered saline (137 mM NaCl , 2.7 mM KCL , $10\text{ mM Na}_2\text{HPO}_4$ and $1.8\text{ mM KH}_2\text{PO}_4$, pH 7.4.) Fluorescence measurements were performed at 360 nm excitation and 460 nm emission (Microplate reader, Synergy-4, Biotek Instruments, Winooski, VT, USA) using solutions of ZnCl_2 for calibration. Data were expressed as relative fluorescence units (RFU)/mg proteins.

The activity of arachidonate-dependent cyclooxygenase (COX) was assessed by a fluorescent assay as published previously [26]. Briefly, $25\text{ }\mu\text{L}$ of S15 fraction was added to $175\text{ }\mu\text{L}$ of reaction mix containing $50\text{ }\mu\text{M}$ arachidonic acid, $1\text{ }\mu\text{M}$ dichlorofluorescein and $0.1\text{ }\mu\text{g/mL}$ horseradish peroxidase in the following assay buffer: $50\text{ mM Tris-acetate}$, 0.5 mM EDTA and 0.05% Tween-20 at pH 8.0. The enzymatic reactions were carried out at room temperature and the time-dependent formation of fluorescein was measured at 485 nm excitation and 528 nm emission at a rate of 3 min for 40 min (Synergy 4, Biotek Instruments, Winooski, VT, USA). The data were expressed as the increase in RFU/min/mg proteins.

Neural activity was estimated by acetylcholinesterase (AChE) activity in the S15 fraction. The assay was performed by using acetylthiocholine as a substrate and Ellman's reagent for thiol groups detection (absorbance 412 nm) as previously described [27]. Calibration was achieved with standard preparations of reduced glutathione. Results were expressed as absorbance increase/min/mg proteins.

The levels of proteins targeted to the ubiquitin-proteasome pathway were quantified by a poly-ubiquitinated protein enzyme-linked immunosorbent assay (ELISA) in the S15 fraction as described in a previous study [28]. Briefly, blanks, standards of poly-ubiquitin (Ub2-7, K48-linked, Enzo Life Sciences, Farmingdale, NY, USA) and S15 fractions ($1\text{ }\mu\text{g}$ total proteins per well) were prepared in coating buffer and incubated overnight in microplate Immulon-4 at $4\text{ }^{\circ}\text{C}$. After three washing steps in $100\text{ }\mu\text{L}$ PBS, the blocking buffer (1% BSA in PBS) was added to each well for 1 h at room temperature. The microplate was washed twice, then the primary antibody (ubiquitin lys48-specific, clone Apu2; EMD Millipore, Billerica, MA, USA) diluted 1/2000 in PBS-0.5% BSA was added for 3 h. After the incubation period, the wells were washed thrice in PBS and the secondary antibody (anti-rabbit IgG-HRP conjugate; ADI-SAB-300, Enzo, Farmingdale, NY, USA) diluted 1/5000 in PBS-0.05% BSA was incubated for another hour. After three washing steps in PBS, peroxidase activity was determined using a highly sensitive chemiluminescence detection kit (BM Chemiluminescence ELISA substrate, Roche Diagnostics, QC, Canada). Data were expressed as ng of polyubiquitin/mg proteins.

2.5. Data Analysis

The exposure experiments were performed with $N = 30$ mussels for each of the seven treatment groups: controls, nAg, nCeO, nCuO, nZnO, Mix50 and Mix200. The exposure experiment was repeated twice. Sub-groups of 10 mussels in each treatment group were randomly selected for bioaccumulation, air survival and biomarkers analyses. Replication was achieved by having 10 individual mussels per experiment (repeated two times) for bioaccumulation, air survival and biomarker assessments. This approach involved low replication of the experiment repetition level as a compromise (time and budget), giving the high number of biomarker endpoints. Data normality and homogeneity of variance were determined by the Shapiro–Wilks and Bartlett tests, respectively. The data were then subjected to an analysis of variance followed by the Tuckey test as the *post hoc* test to seek out difference between the controls or between the individual nanoparticles and their mixture counterpart. Correlation, principal component and discriminant function analyses were also performed to seek out relationships between the data and determine difference between individual nanoparticles and their mixtures. Significance was set at $p < 0.05$. All statistical analyses were performed with the SysStat software package (version 13.2, San Jose, CA, USA).

3. Results

The nanoparticles were all prepared in MilliQ water and were between 50 and 100 nm mean diameter (Table 1). The mean diameters of the nanoparticles were 51, 47, 64, and 63 nm for nAg, nCeO, nCuO and nZnO, indicating that the nanoparticles were in the same size range. The Zeta potential for these nanoparticle suspensions in aquarium water were -48 , -14.7 , -12.4 , and -22.6 mV for nAg, nCeO, nCuO and nZnO, respectively. This suggests that nAg and nCuO would be the least and most sensitive to surface charge cancellation and formation of aggregates. Based on previous experiments and analysis with dynamic light scattering, the mean diameter of the nanoparticles did not change after one hour in aquarium water but tended to form aggregates after 48 h between 100 and 450 nm size range [28–31]. However, the changes in the diameter size were not determined in the mixtures in the present study. There was no change in pH and conductivity throughout the exposure period (time 0, 48 and 96 h).

The total levels of Ag, Ce, Cu, and Zn were determined in the soft tissues of mussels (Figure 1). The levels of Ag were significantly increased ($p > 0.01$) in mussels exposed to nAg (50 $\mu\text{g/L}$ as total Ag), Mix 50 (12.5 $\mu\text{g/L}$ of each the four nanoparticles) and Mix 200 (50 $\mu\text{g/L}$ for each of the four nanoparticles). The levels of Ag were about 4.5 times lower in the Mix50 group (corresponding to 12.5 $\mu\text{g/L}$) suggesting that the bioavailability of nAg was not affected in the presence of the other Cu, Ce, and ZnO nanoparticles. A metal tissue accumulation factor was calculated based on the following relationship: concentration in tissues ($\mu\text{g/kg}$)/Concentration in water ($\mu\text{g/L}$) was 150, 160 and 140 L/kg for nAg alone, Mix50 and Mix200, respectively. The levels of Ce were also significantly increased in mussels exposed to nCeO alone ($p < 0.01$), Mix50 and Mix200 groups although they were detected at the ng/g range (Figure 1). The levels of Ce were detected in controls at concentration of 9 ng/g and significantly rose to 149, 94 and 485 ng/g in mussels exposed to nCeO alone, Mix50 and Mix200, respectively. The metal tissue accumulation factor was thus 0.003, 0.007 and 0.01, suggesting that nCeO was less available than the other nanoparticles, albeit more available in the presence of the other nanoparticles. The levels of total Cu in mussels were also determined (Figure 1). Cu was present in controls at 0.30 $\mu\text{g/g}$ and was significantly increased ($p < 0.05$) in mussels exposed to nCuO alone (0.47 $\mu\text{g/g}$), Mix50 (0.45 $\mu\text{g/g}$) and Mix200 (0.59 $\mu\text{g/g}$). Total Cu levels were not significantly different ($p > 0.05$) in the Mix200 and Mix50 groups compared to nCuO alone group, suggesting no mixture interactions. The metal tissue accumulation factor was 9.4, 9 and 12, suggesting that nCuO in tissues was higher in the presence of the other nanoparticles. Correlation analysis revealed that tissue Cu levels were significantly related with total Ce in tissues ($r = 0.59$) and Ag in tissues ($r = 0.52$). The levels of total Zn were also determined in mussels exposed to the four inorganic nanoparticles and the mixtures (Figure 1). As with Cu and Ce, Zn was found in controls (2 $\mu\text{g/g}$) and the levels were significantly

increased in mussels exposed to nZnO (3.2 $\mu\text{g/g}$), Mix50 (2.5 $\mu\text{g/g}$) and Mix200 (3.8 $\mu\text{g/g}$). There was no significant difference between mussels exposed to nZnO alone and Mix200, but the levels of total Zn were significantly lower to the Mix50 group corresponding to 12.5 $\mu\text{g/L}$. The metal tissue accumulation factor for Zn were 64, 136 and 76 in mussels exposed nZnO alone, Mix50 and Mix200, suggesting that metal availability was not affected in the presence of the other nanoparticles in Mix200, i.e., with the mixture containing the same amount of added Zn (50 $\mu\text{g/L}$). However, in the Mix50 corresponding to 12.5 $\mu\text{g/L}$ added Zn, bioaccumulation was enhanced, suggesting that availability also depends on concentration for Zn. Correlation analysis revealed that the total Zn levels in tissues were significantly correlated with Cu ($r = 0.54$), Ce ($r = 0.53$) and Ag ($r = 0.36$).

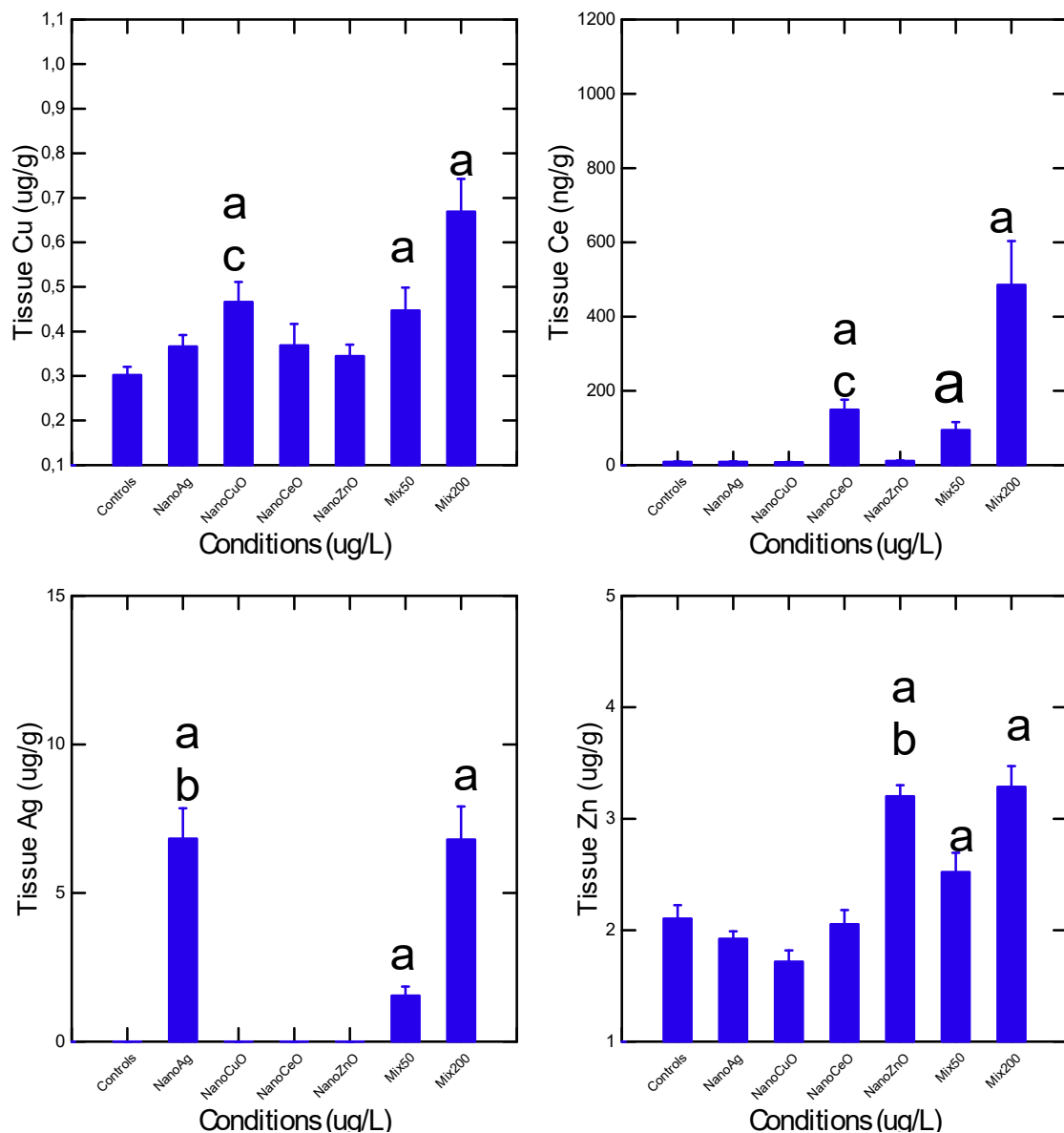


Figure 1. Bioavailability of inorganic nanoparticles alone and in mixtures. Mussels tissues were analyzed for Ag, Ce, Cu and Zn levels following a 12 h depuration step in clean aquarium water. The data represent the mean with the standard deviation. The letters a denotes a significant difference to controls, the letter b denotes significant effect from the Mix50, and c denotes significant difference from Mix200.

The morphological parameters, air survival and weight loss at time of death were also determined in mussels (Table 2). No clear response pattern was found, although mussel mass was significantly increased ($p < 0.05$) in mussels exposed to nAg only, but not in the mixtures. The soft tissue weight/shell length ratio was increased in Mix500 exposure group only and not by any of the individual nanoparticles. No significant changes ($p > 0.05$) in air survival time were observed, but the maximal weight loss during the air survival challenge was significantly decreased ($p < 0.05$) to 0.6-fold in the nCuO group compared to controls. Correlation analysis revealed that air survival time was significantly correlated with weight loss ($r = -0.49$), Zn levels ($r = 0.27$) and tissue Cu levels ($r = 0.37$). The condition factor (mussel weight/shell length ratio) was significantly correlated with Cu ($r = -0.28$) and Ce ($r = -0.48$).

Table 2. Morphological characteristics and air survival time of mussels.

Condition	Mussel Mass (g)	Soft Weight/Length	Condition Factor (g/Length)	Air Survival (Days)	Weight Loss (%)
Control	2.14 ± 0.07	0.107 ± 0.007	0.086 ± 0.004	3.7 ± 0.4	8.5 ± 1.4
nAg	2.45 ± 0.08 ^{abc}	0.109 ± 0.006 ^c	0.093 ± 0.004	3.8 ± 0.49	7.33 ± 1.4
nCuO	2.09 ± 0.05	0.112 ± 0.004 ^c	0.083 ± 0.004	3.7 ± 0.4	5 ± 1.4 ^a
nCeO	2.16 ± 0.1	0.120 ± 0.006 ^c	0.084 ± 0.004	4.4 ± 0.45	7.02 ± 1.5
nZnO	2.29 ± 0.09	0.113 ± 0.005 ^c	0.088 ± 0.004	4.0 ± 0.48	7.44 ± 1.4
Mix (50 ug/L)	2.22 ± 0.09	0.117 ± 0.006	0.087 ± 0.004	4.1 ± 0.45	6.57 ± 1.5
Mix (200 ug/L)	2.06 ± 0.08	0.130 ± 0.006 ^a	0.076 ± 0.004	4.2 ± 0.42	6.12 ± 1.45

The data represent the mean with the standard error. The letter a indicates significance to controls, the letter b indicates difference from the Mix50 and the letter c indicates difference from the Mix200.

Oxidative stress status was examined by following changes in arachidonate COX activity and LPO levels (Figure 2). For COX activity, the levels were significantly lower ($p < 0.01$) in the mussels exposed to nCuO compared to the controls. The activity was also somewhat lower in mussels exposed to nAg, but this “anti-inflammatory” effect was abolished when compared to the mixtures Mix50 and Mix200, i.e., returning to control values ($p > 0.05$). With respect to LPO levels, no significant changes ($p > 0.05$) were observed, with the exception of reduced levels in mussels exposed to nZnO compared to controls. However, this antioxidant effect was lost in the presence of the mixtures Mix50 and Mix200. Correlation analysis revealed that COX activity was significantly correlated with air survival ($r = -0.24$). LPO levels were correlated with COX activity ($r = -0.38$) (Table 3). DNA strand break levels were significantly decreased ($p < 0.05$) in the Mix200 compared to controls, suggesting decreased repair activity and DNA turnover (Figure 3). Levels of DNA breaks in mussels exposed to the Mix200 were significantly lower ($p < 0.05$) than mussels exposed to nAg and nCuO alone. Correlation analysis revealed that DNA strand breaks were significantly correlated with total Ce ($r = -0.24$) and total Zn ($r = -0.27$) in tissues (Table 3). The levels of labile intracellular Zn and damaged protein turnover (protein–ubiquitin) were determined (Figure 4A). The levels of intracellular Zn were influenced by most nanoparticles. With respect to controls, labile Zn levels were significantly reduced ($p < 0.05$) by the nCuO group and increased by the nZnO group. The levels of labile Zn in mussels exposed to either nAg or nCeO alone were significantly lower ($p < 0.05$) compared to the Mix50 group. The increase in labile Zn by nZnO group was abolished in the Mix200 group, suggesting antagonism. Correlation analysis revealed that labile Zn was correlated with COX activity ($r = 0.43$) and total Zn levels ($r = 0.52$).

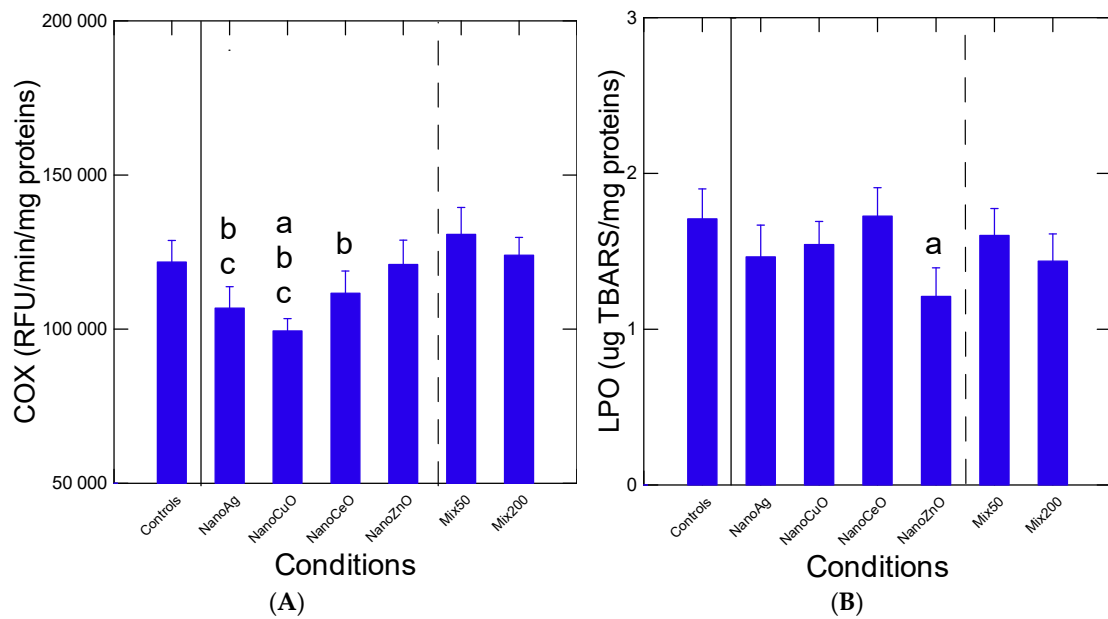


Figure 2. Oxidative stress of nanoparticle mixtures in zebra mussels. Oxidative stress was measured by COX activity (A) and LPO (B). The data represent the mean with the standard deviation. The letters a denotes a significant difference to controls, the letter b significant effect from the Mix50, and c a significant difference from Mix200.

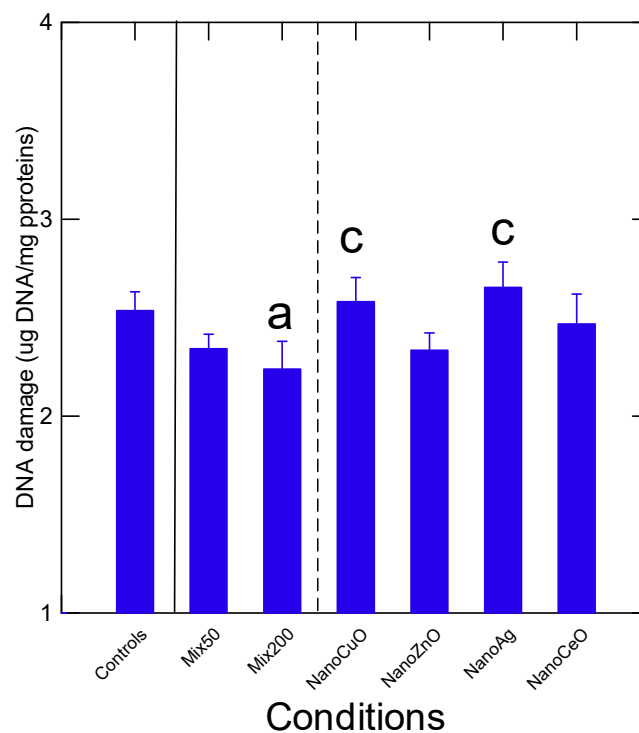


Figure 3. Analysis of DNA strand breaks in mussels exposed to the elemental nanoparticles. The levels of DNA strand breaks were determined by the alkaline DNA precipitation assay. The data represent the mean with the standard deviation. The data represent the mean with the standard deviation. The letters a denotes a significant difference to controls, the letter b significant effect from the Mix50, and c a significant difference from Mix200.

Table 3. Correlation analysis of biomarker data.

	Mass	SFT	CF	Air	WL	LPO	DNA	COX	UB	AChE	Zni	Cu	Ce	Ag	Zn
Mass	1														
SFT	0.43	1													
CF	0.47	0.08	1												
Air	0.18	0.20	0.1	1											
WL	0.03	−0.02	−0.25	−0.49	1										
LPO	−0.02	0.14	0.03	0.08	−0.09	1									
DNA	−0.06	0.06	0.23	−0.15	−0.14	−0.05	1								
COX	−0.12	−0.12	−0.08	−0.25	0.1	−0.38	−0.05	1							
UB	−0.08	0.15	−0.11	−0.13	0.03	0.23	−0.23	0.29	1						
AChE	−0.15	−0.13	−0.09	−0.17	0.09	−0.62	0.22	0.21	−0.12	1					
Zni	0.17	0.13	0.04	−0.07	0.2	−0.16	0.04	0.43	0.03	0.1	1				
Cu	−0.07	0.17	−0.28	0.37	−0.2	−0.08	−0.14	−0.16	0.05	−0.07	−0.22	1			
Ce	−0.17	0.12	−0.48	0.19	0.01	−0.1	−0.24	0.02	0.03	0.11	0.05	0.66	1		
Ag	0.09	0.19	−0.19	0.17	0.01	−0.1	−0.1	−0.09	0.06	0.10	−0.04	0.52	0.59	1	
Zn	0.08	0.17	−0.16	0.27	0.07	0.18	−0.27	0.12	0.12	−0.08	0.52	0.54	0.53	0.36	1

SFT: soft tissue weight; CF: condition factor (mussel mass/shell length); Air: sir time survival; WL: weight loss; Zni: labile Zn in the s15 fraction of the homogenate. Significant correlations are highlighted in bold ($p < 0.05$).

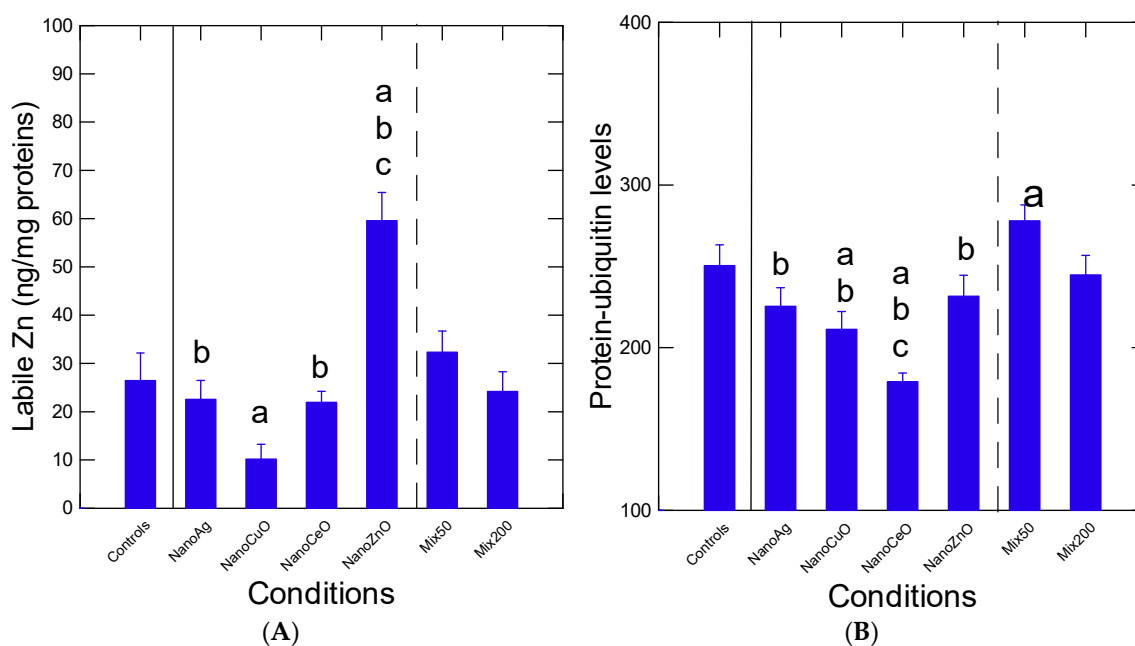


Figure 4. Labile Zn and protein ubiquitin levels in mussels exposed to nanoparticles and their mixture. Labile Zn (A) and Protein-ubiquitin (B) levels were determined in mussels. The data represent the mean with the standard deviation. The letters a denotes a significant difference to controls, the letter b a significant effect from the Mix50 and c a significant difference from Mix200.

Changes in damaged protein turnover were studied by following protein-bound UB levels (Figure 4B). The data revealed that levels of UB–protein were significantly decreased ($p < 0.05$) by nCuO and nCeO and increased by the Mix50 group with respect to control mussels (Figure 4B). The decrease in protein–UB levels in mussels exposed to nCeO alone was lost in the Mix200. The levels in protein–UB levels in mussels exposed to nAg and nZnO were significantly lower ($p < 0.05$) in mussels exposed to the Mix50 group. Protein–UB levels were somewhat correlated with DNA damage ($r = -0.23$), COX activity ($r = 0.29$) and total Zn in tissues ($r = 0.31$). Neural activity was examined by following AChE activity and revealed no significant changes ($p > 0.05$) by the individual nanoparticles and the two mixtures (Figure 5). Correlation analysis revealed that AChE activity was significantly correlated with LPO ($r = -0.62$).

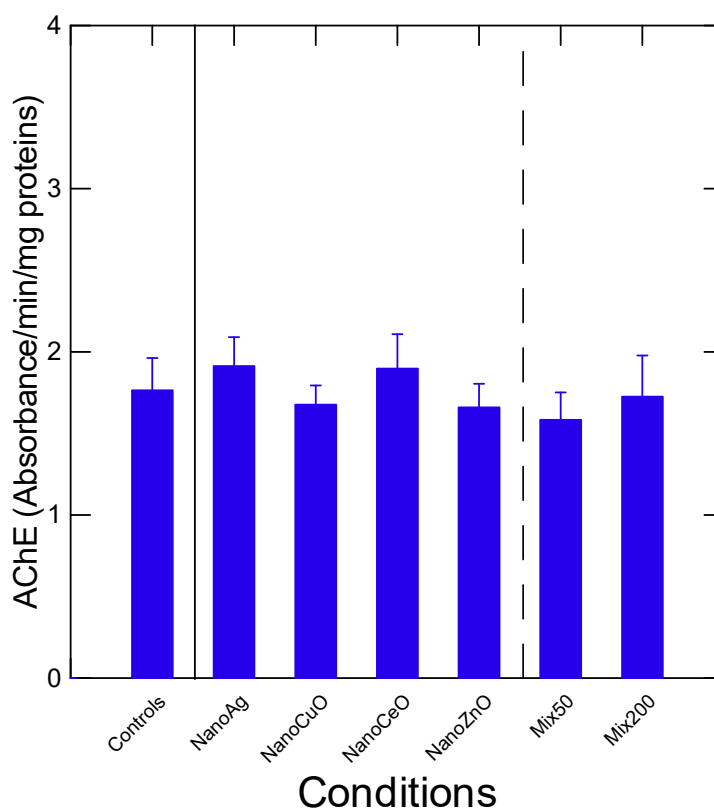
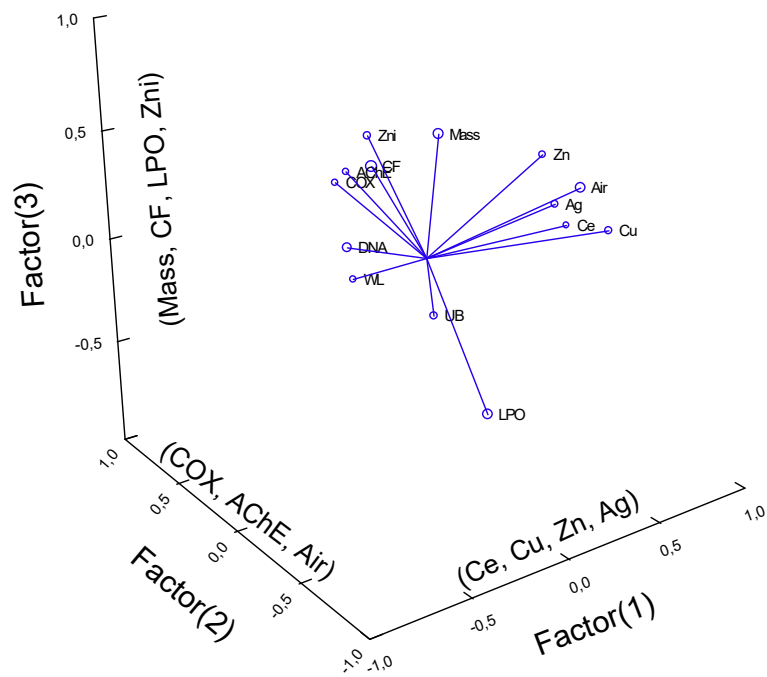
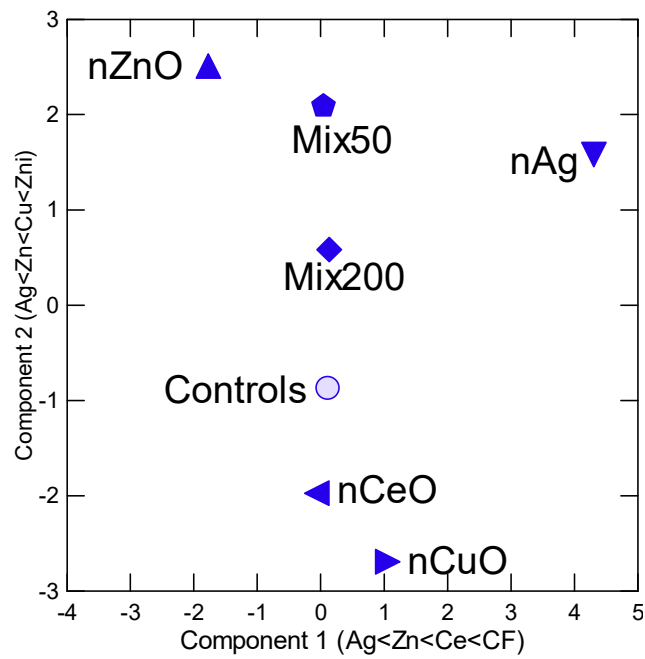


Figure 5. AChE activity in freshwater mussels exposed to nanoparticles and their mixtures. The data represent the mean with the standard deviation.

In the attempt to provide a general view of the various responses in mussels exposed to the nanoparticles and their mixtures, factorial and discriminant function analyses were performed (Figure 6). Factorial analysis revealed that 72% of the total variance was explained by three factors (Figure 6A). The biomarkers with the highest factorial weights were tissue levels of Ce, Cu, Zn and Ag, mass, CF, COX, LPO, Zni (intracellular labile Zn) and AChE. Air survival was closely associated with Ag, Ce, Cu and Zn tissue levels. Protein damage (UB) was negatively associated with CF, Age, COX and AChE activity. We also performed a multiple regression analysis to determine the endpoints that best predicted air-time survival. The analysis revealed a multiple $r = 0.59$ with the following independent variables: weight loss ($\beta = -0.16$; $p < 0.001$), protein-UB ($\beta = -0.01$; $p < 0.05$) and total Zn in tissues ($\beta = 0.7$; $p < 0.001$) and a constant (5.2 ; $p < 0.001$). This suggests that damaged protein turnover activity, weight loss during air emersion (dehydration rate) could reduce air survival time, while increased Zn in tissues was beneficial, i.e., increased resistance to air emersion. Discriminant function analysis was also performed to identify the most important biomarkers responsible for the mixture effects of inorganic nanoparticles (Figure 6B). The analysis revealed that the tissue metal levels (Ag, Ce, Cu and Zn), CF (mussel weight/shell length) and labile Zni were the most important biomarkers for site discrimination. If we remove the biomarkers of exposure (Ag, Ce, Cu and Zn levels), the following biomarkers of effects were the most important: labile Zni, CF, protein-UB and DNA damage. The site classification efficiency was much lower at 32% and the effects of nAg and nCuO were indiscriminate from the Mix200 effects and were closer to the responses observed in controls (antagonist interactions).



(A)



(B)

Figure 6. Multivariate analysis of biomarker data. The biomarker data were analysed by factorial (principal component: (A)) and discriminant function (B) analyses. For factorial analysis, the biomarkers with the highest factorial weights are indicated at each axis. For discriminant function analysis, the mean classification efficiency was 73% and the first 4 biomarkers with high factorial weights are included in both axes.

4. Discussion

The toxicity of the Ag, Ce, Cu, and Zn nanoparticles was examined individually and in mixtures in bivalves. To best of our knowledge, virtually no studies examined the combined/cumulative effects of inorganic nanoparticles in aquatic animals, which should occur in contaminated environments. In zebra mussels exposed to dissolved Ag(I), Cd(II), Pd(II) and Pt(II) elements, no differences in accumulation were observed in *Dreissena polymorpha* [32]. In the present study, the accumulation of Ag, Ce, Cu and Zn nanoparticles was examined individually at 50 µg/L and in two mixtures: Mix50, where the sum of the four nanoparticles (uncoated) equals 50 µg/L (12.5 µg/L each elemental nanoparticle) and Mix200, where the four nanoparticles at 50 µg/L concentration each equals 200 µg/L. While nAg and nZnO accumulated in mussel tissues independently, alone and in mixtures, nCuO and nCeO accumulation was enhanced in the mixture (Mix200) compared to the nanoparticles alone. This suggests that metal tissue accumulation factor of inorganic nanoparticles could also be influenced by other nanoparticles as with nCuO and nCeO, although bioavailability factors were relatively low for nCeO (<1 L/Kg) compared to the other nanoparticles. Increased availability was observed with exogenous ligands such as natural organic matter for nZnO by preventing aggregation [33,34]. However, it was not determined if aggregation changed in the nanoparticle mixtures. In the presence of natural organic matter, the toxicity of cadmium-based quantum dots was reduced in *Daphnia magna*. Interestingly, the organic matter from a municipal effluent was less effective in reducing toxicity compared to the organic matter from lake origin. It was suggested that the organic matter forms a corona to stabilize the nanoparticle against aggregation, thereby influencing metal availability and toxicity. In addition to exogenous ligands, endogenous ligands such as proteins or lipids could also interact at the surface of nanoparticles. For example, the Cu,Zn-superoxide dismutase and ubiquitin (a tag for damaged protein turnover) formed a corona at the surface of Ce oxide nanoparticle [35,36]. This interaction could deplete ubiquitin levels in cells and prevent binding to damaged protein for turnover in cells. Interestingly, nCuO and nCeO reduced protein–ubiquitin levels when presented alone to the mussels, whereas this effect was seemingly lost in the mixtures. This suggests that nCuO or nCeO in the presence of other nanomaterials could increase turnover of damaged protein. Increased protein–UB levels were significantly associated with COX activity, decreased DNA strand breaks (repair) and total Zn levels in cells. The antioxidant and immunoprotective properties of Zn in tissues were previously recognized [37] where inflammation could be controlled by Zn levels in cells [38]. This is also in keeping with the positive correlation between labile Zni and COX activity.

Based on discriminant function analysis, the effects of nAg and nZnO differed the most from controls and the other nanoparticles (nCeO, nCuO). The Mix50 and Mix200 response patterns differed from nAg and nZnO and were closer to controls, suggesting suppression (antagonisms) of the effects of the nanoparticle mixtures. Exposure of the Mediterranean mussel *Mytilus galloprovincialis* to nAg released from nAg-embedded clothing revealed that this nanoparticle was still bioavailable and toxic [39]. Mussels exposed to an environmentally realistic concentration of nAg (1–10 µg/L) showed increased gill LPO, gill metallothioneins and hemocyte micronuclei levels. Although no signs of DNA damage and oxidative damage (LPO) were obtained in the present study, the levels of labile Zni, a surrogate for metallothioneins and oxidative stress [25,39], were only increased in mussels exposed to nZnO. In marine mussels exposed to either 10 mg/L nCeO or nZnO, they accumulated 62 µg/g Ce and 880 µg/g Ce, giving metal tissue accumulation factors of 6 and 88 for Ce and Zn, respectively [40]. These values were higher than those obtained in the present study with Ce but similar for Zn with a freshwater species, albeit with a low exposure concentration of 50 µg/L: 0.003 and 64 for Ce and Zn respectively. This suggests that the bioavailability of inorganic nanoparticles is concentration-dependent and depends on the salinity of the marine/freshwaters. It is possible that the high salt content of sea water could have favored aggregation, which are retained longer in mussel's digestive system and gills. Interestingly, the metal tissue accumulation factor was increased three-fold in the mixtures for nCeO (0.003 to 0.01-fold) and not for nZnO. With respect to nCuO, exposure of marine mussels to 10 µg/L nCuO led to the accumulation of 20 mg/kg, giving a metal tissue

accumulation factor of 2000 in the digestive gland [41]. These values were much higher than those obtained in the present study with freshwater. Aggregation seems to be a key factor for the uptake in mussels, since they are filter feeders. A previous study comparing the toxicity of nCuO and dissolved Cu(II) in the marine mussel *Mytilus galloprovincialis* showed that the toxic action of nCuO differed from Cu(II) [42]. Indeed, nCuO-induced oxidative stress in gills of mussels saturating the antioxidant defense system, while Cu(II) increased antioxidant enzyme activities. On the other hand, both forms of Cu increased metallothioneins and LPO in gills. It is possible that the differences observed in these responses result from dephased responses in time where the molecular effects of nCuO would be produced earlier than Cu(II) and would tend to follow an inverted U dose response often found in molecular biomarker signals [43,44]. In another study with *Scrobicularia plana* clams, nCuO was completely aggregated in sea water with the absence of changes in labile Cu levels [45]. Biomarkers of oxidative stress were nevertheless observed such as superoxide dismutase, catalase and glutathione S-transferase. These effects were related to nCuO but not to the soluble form of Cu(II). In a previous study with *Elliptio complanata* mussels exposed to an equivalent 1–10 µg/L concentration of nZnO for 21 days, no significant accumulation of total zinc occurred [29] (Gagnon et al., 2016). However, levels of labile Zn, metallothioneins and protein-ubiquitination were significantly increased suggesting a mobilization of Zn in cells by nZnO. In the present study, significant accumulation occurred in mussels exposed to 50 µg/L nZnO individually and in both mixtures. However, labile Zn levels only increased when presented alone (not observed in the mixtures). This raises the possibility that labile Zn is released either from nZnO or oxidative processes, although this is unlikely for the latter given the lack of LPO. In the presence of other nanoparticles, labile Zn is lost, perhaps through binding to redox enzymes and perhaps with other nanoparticles. Zinc is an essential trace metal involved in redox homeostasis in cells and has antioxidant properties compared to other metals such as copper and iron [46]. It is a key element for hundreds of enzymes at the level of catalytic site activity, coactivators of enzymes and stabilizing protein conformation [47] (Vallee and Falchuk, 1993).

5. Conclusions

In conclusion, freshwater mussels accumulated the inorganic nanoparticles when exposed individually and in mixtures. With the exception of nCeO (enhanced accumulation in mixtures) accumulation was not significantly affected by nanoparticles in mixture. Labile Zn levels in homogenate extracts were significantly increased individually but not in mixtures and were correlated with total Zn uptake in tissues of mussels. A decrease in labile Zn levels was found in mussels exposed to nCuO alone but not in mixtures, suggesting a role in oxidative stress and decreased protein-ubiquitin tagging for protein turnover. The global effects of the mixtures were generally closer to nZnO and nAg and to controls with the MIX200, suggesting antagonist interactions between nanoparticles. The data presented in this study are preliminary given the study design (the experiments were repeated twice) but suggest that the resulting effects of nanoparticles could be influenced by the presence of other nanoparticles in freshwater mussels.

Author Contributions: Conceptualization, planning of experiments, and writing original manuscript: F.G.; biomarkers and data analysis, J.A.; nanoparticle characterization by dynamic light scattering, C.P.; mass spectrometry analysis for bioaccumulation of elements in organisms, P.T.; validation of chemistry analysis and manuscript data analysis and interpretation, K.J.W. and C.G. All authors have read and agreed to the published version of the manuscript.

Funding: This project was funded by the Chemical Management Plan of Environment and Climate Change Canada.

Acknowledgments: The authors acknowledge the technical assistance of Joanna Kowalcik.

Conflicts of Interest: The authors declare no conflict of interest in the preparation and review of this research article.

References

1. Malhotra, N.; Ger, T.R.; Uapipatanakul, B.; Huang, J.C.; Chen, K.H.; Hsiao, C.D. Review of Copper and Copper Nanoparticle Toxicity in Fish. *Nanomaterials* **2020**, *10*, 1126. [[CrossRef](#)] [[PubMed](#)]
2. You, G.; Hou, J.; Xu, Y.; Miao, L.; Ao, Y.; Xing, B. Surface Properties and Environmental Transformations Controlling the Bioaccumulation and Toxicity of Cerium Oxide Nanoparticles: A Critical Review. *Rev. Environ. Contam. Toxicol.* **2020**. [[CrossRef](#)]
3. Bodó, K.; Baranzini, N.; Girardello, R.; Kokhanyuk, B.; Németh, P.; Hayashi, Y.; Grimaldi, A.; Engelmann, P. Nanomaterials and Annelid Immunity: A Comparative Survey to Reveal the Common Stress and Defense Responses of Two Sentinel Species to Nanomaterials in the Environment. *Biology* **2020**, *23*, 307. [[CrossRef](#)] [[PubMed](#)]
4. Holeton, C.; Chambers, P.A.; Grace, L. Wastewater release and its impacts on Canadian waters. *Can. J. Fish. Aquat. Sci.* **2011**, *68*, 1836–1859. [[CrossRef](#)]
5. Zhang, C.; Hu, Z.; Deng, Z. Silver nanoparticles in aquatic environments: Physicochemical behavior and antimicrobial mechanisms. *Water Res.* **2016**, *88*, 403–427. [[CrossRef](#)]
6. Polesel, F.; Farkas, J.; Kjos, M.; Carvalho, P.A.; Flores-Alsina, X.; Gernaey, K.V.; Hansen, S.F.; Plósz, B.G.; Booth, A.M. Occurrence, characterisation and fate of (nano) particulate Ti and Ag in two Norwegian wastewater treatment plants. *Water Res.* **2018**, *141*, 19–31. [[CrossRef](#)]
7. Charbgoon, F.; Bin Ahmad, M.; Darroudi, M. Cerium oxide nanoparticles: Green synthesis and biological applications. *Int. J. Nanomed.* **2017**, *12*, 1401–1413. [[CrossRef](#)]
8. Eom, H.J.; Choi, J. Oxidative stress of CeO₂ nanoparticles via p38-Nrf-2 signaling pathway in human bronchial epithelial cell, Beas-2B. *Toxicol. Lett.* **2009**, *187*, 77–83. [[CrossRef](#)]
9. Kumar, M.V.; Babu, A.V.; Kumar, P.R. Influence of metal based cerium oxide nanoparticle additive on performance, combustion, and emissions with biodiesel in diesel engine. *Environ. Sci. Pollut. Res. Int.* **2019**, *26*, 7651–7664. [[CrossRef](#)]
10. Mohajerani, A.; Burnett, L.; Smith, J.V.; Kurmus, H.; Milas, J.; Arulrajah, A.; Horpibulsuk, S.; Kadir, A.A. Nanoparticles in Construction Materials and Other Applications, and Implications of Nanoparticle Use. *Materials* **2019**, *12*, 3052. [[CrossRef](#)]
11. Cole, C.; Shyr, T.; Ou-Yang, H. Metal oxide sunscreens protect skin by absorption, not by reflection or scattering. *Photodermatol. Photoimmunol. Photomed.* **2016**, *32*, 5–10. [[CrossRef](#)] [[PubMed](#)]
12. Canesi, L.; Ciacci, C.; Fabbri, R.; Marcomini, A.; Pojana, G.; Gallo, G. Bivalve molluscs as a unique target group for nanoparticle toxicity. *Mar. Environ. Res.* **2012**, *76*, 16–21. [[CrossRef](#)] [[PubMed](#)]
13. Gagné, F.; Gagnon, C.; Blaise, C. Aquatic Nanotoxicology: A review. *Curr. Top. Toxicol.* **2007**, *4*, 51–64.
14. Auclair, J.; Turcotte, P.; Gagnon, C.; Peyrot, C.; Wilkinson, K.J.; Gagné, F. Comparative Toxicity of Copper Oxide Nanoparticles and Dissolved Copper to Freshwater Mussels. *Intern. J. Zool. Investig.* **2019**, *6*, 135–147.
15. Song, L.; Vijver, M.G.; Peijnenburg, W.J.; Galloway, T.S.; Tyler, C.R. A comparative analysis on the in vivo toxicity of copper nanoparticles in three species of freshwater fish. *Chemosphere* **2015**, *139*, 181–189. [[CrossRef](#)]
16. Adam, N.; Schmitt, C.; De Bruyn, L.; Knapen, D.; Blust, R. Aquatic acute species sensitivity distributions of ZnO and CuO nanoparticles. *Sci. Total Environ.* **2015**, *526*, 233–242. [[CrossRef](#)]
17. Mansano, A.S.; Souza, J.P.; Cancino-Bernardi, J.; Venturini, F.P.; Marangoni, V.S.; Zucolotto, V. Toxicity of copper oxide nanoparticles to Neotropical species *Ceriodaphnia silvestrii* and *Hyphessobrycon eques*. *Environ. Pollut.* **2018**, *243*, 723–733. [[CrossRef](#)]
18. Hernández-Moreno, D.; Valdehita, A.; Conde, E.; Rucandio, I.; Navas, J.M.; Fernández-Cruz, M.L. Acute toxic effects caused by the co-exposure of nanoparticles of ZnO and Cu in rainbow trout. *Sci. Total Environ.* **2019**, *687*, 24–33. [[CrossRef](#)]
19. Baalousha, M. Sewage spills are a major source of titanium dioxide engineered (nano)-particles into the environment. *Environ. Sci. Nano* **2019**, *3*. [[CrossRef](#)]
20. Du, P.; Zhang, L.; Ma, Y.; Li, X.; Wang, Z.; Mao, K.; Wang, N.; Li, Y.; He, J.; Zhang, X.; et al. Occurrence and Fate of Heavy Metals in Municipal Wastewater in Heilongjiang Province, China: A Monthly Reconnaissance from 2015 to 2017. *Water* **2020**, *12*, 728. [[CrossRef](#)]
21. Bradford, M.M. A rapid and sensitive method for the quantitation of microgram quantities of protein utilizing the principle of protein-dye binding. *Anal. Biochem.* **1976**, *72*, 248–254. [[CrossRef](#)]

22. Wills, E.D. Evaluation of lipid peroxidation in lipids and biological membranes. In *Biochemical Toxicology: A Practical Approach*; Snell, K., Mullock, B., Eds.; IRL Press: Washington, DC, USA, 1987; p. 127.
23. Olive, P.L. DNA precipitation assay: A rapid and simple method for detecting DNA damage in mammalian cells. *Environ. Mol. Mutagenes.* **1988**, *11*, 487–495. [[CrossRef](#)] [[PubMed](#)]
24. Gagné, F.; Maysinger, D.; André, C.; Blaise, C. Cytotoxicity of aged cadmium-telluride quantum dots to rainbow trout hepatocytes. *Nanotoxicology* **2008**, *2*, 113–120. [[CrossRef](#)]
25. Gagné, F.; Blaise, C. Available intracellular zinc as a potential indicator of heavy metal exposure in rainbow trout hepatocytes. *Environ. Toxicol. Water Qual.* **1996**, *11*, 319–325. [[CrossRef](#)]
26. Gagné, F. *Biochemical Ecotoxicology: Principles and Methods*; Elsevier: Amsterdam, The Netherlands, 2014.
27. Gélinas, M.; Lajeunesse, A.; Gagnon, C.; Gagné, F. Temporal and seasonal variation in acetylcholinesterase activity and glutathione-S-transferase in amphipods collected in mats of *Lyngbya wollei* in the St-Lawrence River (Canada). *Ecotoxicol. Environ. Saf.* **2013**, *94*, 54–59. [[CrossRef](#)]
28. Auclair, J.; André, C.; Peyrot, C.; Wilkinson, K.; Turcotte, P.; Gagnon, C.; Gagné, F. Combined effects of surface waters and CeO nanoparticle in zebra mussels. *Invertebr. Surviv. J.* **2019**, *16*, 152–163.
29. Gagnon, C.; Pilote, M.; Turcotte, P.; André, C.; Gagné, F. Effects of exposure to zinc oxide nanoparticles in freshwater mussels in the presence of municipal effluents. *Invertebr. Surviv. J.* **2016**, *13*, 140–152.
30. Gagnon, C.; Bruneau, A.; Turcotte, P.; Pilote, M.; Gagné, F. Fate of cerium oxide nanoparticles in natural waters and immunotoxicity in exposed rainbow trout. *J. Nanomed. Nanotechnol.* **2018**, *9*, 489–497. [[CrossRef](#)]
31. Auclair, J.; Turcotte, P.; Gagnon, C.; Peyrot, C.; Wilkinson, K.J.; Gagné, F. The influence of surface coatings of silver nanoparticles on the bioavailability and toxicity to *Elliptio complanata* Mussels. *J. Nanomater.* **2019**. [[CrossRef](#)]
32. Yen Le, T.T.; García, M.R.; Grabner, D.; Nachev, M.; Balsa-Canto, E.; Hendriks, A.J.; Zimmermann, S.; Sures, B. Mechanistic simulation of bioconcentration kinetics of waterborne Cd, Ag, Pd, and Pt in the zebra mussel *Dreissena polymorpha*. *Chemosphere* **2020**, *242*, 124967. [[CrossRef](#)]
33. Grillo, R.; Rosa, A.H.; Fraceto, L.F. Engineered nanoparticles and organic matter: A review of the state-of-the-art. *Chemosphere* **2015**, *119*, 608–619. [[CrossRef](#)] [[PubMed](#)]
34. Lee, S.; Kim, K.; Shon, H.K.; Kim, S.D.; Cho, J. Biototoxicity of nanoparticles: Effect of natural organic matter. *J. Nanopart. Res.* **2011**, *13*, 3051–3061. [[CrossRef](#)]
35. Sendra, M.; Volland, M.; Balbi, T.; Fabbri, R.; Yeste, M.P.; Gatica, J.M.; Canesi, L.; Blasco, J. Cytotoxicity of CeO₂ nanoparticles using in vitro assay with *Mytilus galloprovincialis* hemocytes: Relevance of zeta potential, shape and biocorona formation. *Aquat. Toxicol.* **2018**, *200*, 13–20. [[CrossRef](#)] [[PubMed](#)]
36. Ding, F.; Radic, S.; Chen, R.; Chen, P.; Geitner, N.K.; Brown, J.M.; Ke, P.C. Direct observation of a single nanoparticle-ubiquitin corona formation. *Nanoscale* **2013**, *5*, 9162–9169. [[CrossRef](#)] [[PubMed](#)]
37. Poljšak, B.; Fink, R. The Protective Role of Antioxidants in the Defence against ROS/RNS-Mediated Environmental Pollution. *Oxid. Med. Cell. Longev.* **2014**, *2014*, 671539. [[CrossRef](#)] [[PubMed](#)]
38. Olechnowicz, J.; Tinkov, A.; Skalny, A.; Suliburska, J. Zinc status is associated with inflammation, oxidative stress, lipid, and glucose metabolism. *J. Physiol. Sci.* **2018**, *68*, 19–31. [[CrossRef](#)]
39. Ale, A.; Liberatori, G.; Vannuccini, M.L.; Bergami, E.; Ancora, S.; Mariotti, G.; Bianchi, N.; Galdopórpora, J.M.; Desimone, M.F.; Cazenave, J.; et al. Exposure to a nanosilver-enabled consumer product results in similar accumulation and toxicity of silver nanoparticles in the marine mussel *Mytilus galloprovincialis*. *Aquat. Toxicol.* **2019**, *211*, 46–56. [[CrossRef](#)]
40. Montes, M.A.; Hanna, S.K.; Lenihan, H.S.; Keller, A.A. Uptake, accumulation, and biotransformation of metal oxide nanoparticles by a marine suspension-feeder. *J. Hazard. Mater.* **2012**, *225–226*, 139–145. [[CrossRef](#)]
41. Gomes, T.; Pereira, C.G.; Cardoso, C.; Pinheiro, J.P.; Cancio, I.; Bebianno, M.J. Accumulation and toxicity of copper oxide nanoparticles in the digestive gland of *Mytilus galloprovincialis*. *Aquat. Toxicol.* **2012**, *118*, 72–79. [[CrossRef](#)]
42. Gomes, T.; Pinheiro, J.P.; Cancio, I.; Pereira, C.G.; Cardoso, C.; Bebianno, M.J. Effects of copper nanoparticles exposure in the mussel *Mytilus galloprovincialis*. *Environ. Sci. Technol.* **2011**, *45*, 9356–9362. [[CrossRef](#)]
43. Smetanová, S.; Riedl, J.; Zitzkat, D.; Altenburger, R.; Busch, W. High-throughput concentration-response analysis for omics datasets. *Environ. Toxicol. Chem.* **2015**, *34*, 2167–2180. [[CrossRef](#)] [[PubMed](#)]
44. Gagné, F. The wave nature of molecular responses in ecotoxicology. *Curr. Top. Toxicol.* **2016**, *12*, 11–24.

45. Buffet, P.-E.; Tankoua, O.F.; Pan, J.-F.; Berhanu, D.; Herrenknecht, C.; Poirier, L.; Amiard-Triquet, C.; Amiard, J.-C.; Bérard, J.-P.; Risso, C.; et al. Behavioural and biochemical responses of two marine invertebrates *Scrobicularia plana* and *Hediste diversicolor* to copper oxide nanoparticles. *Chemosphere* **2011**, *84*, 166–174. [[CrossRef](#)] [[PubMed](#)]
46. Navarro, J.A.; Schneuwly, S. Copper and Zinc Homeostasis: Lessons from *Drosophila melanogaster*. *Front. Genet.* **2017**, *8*, 223. [[CrossRef](#)]
47. Vallee, B.L.; Falchuk, K.H. The biochemical basis of zinc physiology. *Physiol. Rev.* **1993**, *73*, 79–118. [[CrossRef](#)]

Publisher’s Note: MDPI stays neutral with regard to jurisdictional claims in published maps and institutional affiliations.



© 2020 by the authors. Licensee MDPI, Basel, Switzerland. This article is an open access article distributed under the terms and conditions of the Creative Commons Attribution (CC BY) license (<http://creativecommons.org/licenses/by/4.0/>).